FINE STRUCTURE IN SOLAR DECAMETRIC RADIATION

G. THEJAPPA, Ch. V. SASTRY and N. GOPALSWAMY
Indian Institute of Astrophysics, Bangalore, India,
and Raman Research Institute, Bangalore, India

Abstract Observations and interpretations of some of the fine structure in decametric solar radio emission —such as (1) the time structure of type III bursts, (2) absorption bursts, and (3) slowly drifting spikes —are presented. Physical parameters—such as the electron temperature, the characteristics of collisionless shocks, and the coronal magnetic field—are estimated.

INTRODUCTION

Even though there are a number of observed features at decameter wavelengths, only three distinct features will be presented here: (1) the time structure of solar decameter type III radios bursts, (2) decametric absorption bursts, and (3) slowing drifting spikes.

The usual time profile of a type III burst is characterized by a sharp rise, followed by an exponential type of decay. If the decay is due to collisional damping, then one can calculate the kinetic temperature of the corona where the bursts originate. During the course of our observations of storm type III bursts (Thejappa and Sastry, 1982), we found that the time profiles of these bursts can take a variety of forms; three distinct profiles are presented here. They are profiles where (1) the intensity rises to a small but steady value before the onset of the main burst, (2) the intensity of the main burst reduces to a finite level and remains steady before it decays to the base level, (3) the steady state is present during the rise as well as the decay phase of the main burst.

Fast microstructure in solar radio emission is quite well known in the wavelength range from a few millimeters to decameters (Slottje, 1972, 1978; Sastry, 1973; etc.). Slottje (1972) described peculiar absorptions of the background continuum at meter wavelengths detected with the Utrecht radio spectrograph. During the course of our observations of the microstructure of the decametric continuum, we have detected many interesting absorption features. The characteristics of these absorption features are found to be different from those at short wavelengths (Sastry et al., 1983; Gopalswamy et al., 1983). A summary of the observations and a suggested model are presented.

Various authors have studied narrow-band short-duration slowly moving spikes in other wavelengths (Elgaroy, 1977). Slowly drifting spikes in decametric regions are studied in this paper.

EQUIPMENT

The observations were made with the NS array of the Gauribidanur radio telescope (latitude 13° 36' 12" N, longitude 77° 26' 07" E) and a multichannel receiver. The NS array has a collecting area of approximately 9000 m^2 and beam widths of 15° and 0.5° in the EW and NS directions, respectively. The central frequency of the receiving system is 34.5 MHz. The separation between channels is 50 KHz and the bandwidth of each channel is 15 KHz. The time constant used is 10 ms. The minimum detectable flux density is about 1 SFU. The data were recorded both in analogue and digital forms. The present number of channels is sixteen. The radiometer was operated for about an hour around the local noon during periods of enhanced solar radio emission.

OBSERVATIONS AND INTERPRETATION

Time Structure of Solar Decameter Type III Radio Bursts

We have already reported some of our observations on storm bursts, which are mainly of short duration ($\sim$ 1 s) and narrow band (Sastry 1969, 1971, 1972, 1973). In this study, we consider time profiles of bursts whose total duration lies between 10 and 20 s as well as the short duration bursts. Figure 1 shows typical examples of the type III bursts studied here. In figure 1a, one can see that the intensity rises to about 20 percent of the level of the main peak and remains reasonably steady for a period of about 4 s before the onset of the main burst; we designate this a type A profile. Another type of burst, in which the intensity decays to about 30% of the main peak level and remains steady for a period of 2 s before it decays to

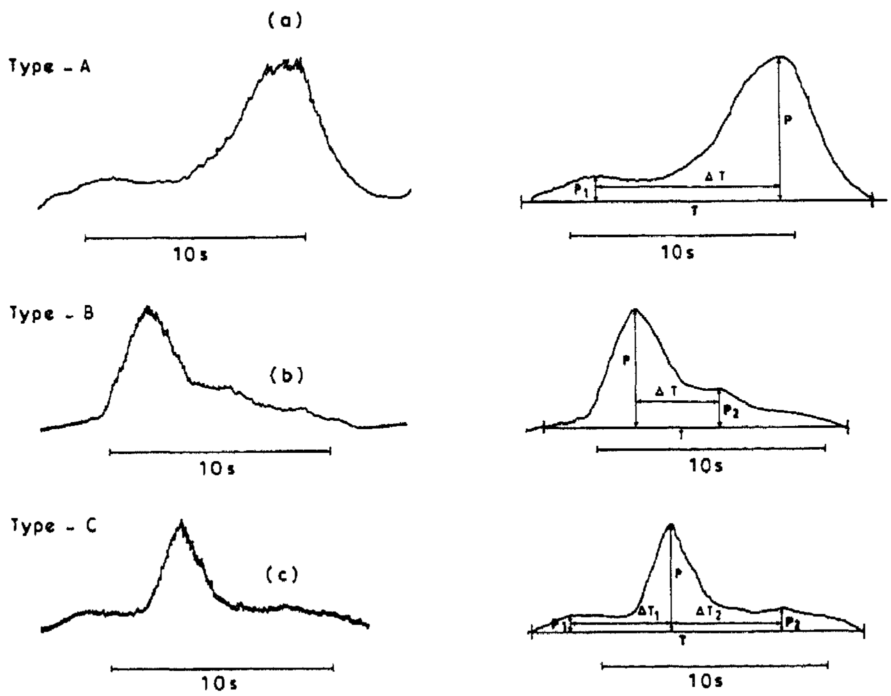

Figure 1. Typical examples of type III burst profiles and the definition of burst parameters.

the base level, is shown in figure 1b and is designated a type B profile. In figure 1c, there is a small but steady rise in intensity for a period of 3 s before the onset of the main burst; also, the main burst decays to a constant level of about 20 percent of the main peak and remains steady for a period of 3 s—we call this a type C profile. Out of the 165 bursts studied, 34 percent belong to type A, 45 percent to type B, and 21 percent to type C profiles. We have measured the various characteristics of these bursts (figure 1) that are of interest to us in the following discussion.

It has been found that the duration of type A profiles lies in the range 14-16 s; that for type B, 10-15 s; and that for type C is $\geq$ 18 s. For type A profiles, ΔT, the time interval between the peak of the main burst and the onset of the steady level is about 5-6 s, whereas it lies between 3 and 6 s for type B profiles. In the case of type C profiles, ΔT_1 (the interval between the main peak and the onset of the steady level) ranges from 5 to 7 s and ΔT_2 (the interval between the main peak and the start of decay of the steady level) is $\leq$ 8 s. The two amplitude ratios—(1) the level of the pre-rise to that of the main peak P_1/P and (2) the level to which the main burst decays and remains steady to the level of the main peak P_2/P—lie in the range 0.1 to 0.3 in all the profiles. Following the procedure of Aubier and Boischot (1972), we have measured the decay constants of the main burst (τ_1) and also that of the final decay of the steady level (τ_2). Note that only τ_1 is present in the case of type A profiles. It has been found that decay constants τ_1 and τ_2 lie in the range 1-4 s for all three types of profiles. There is no strong correlation between τ_1 and the duration of the exciter. Also, τ_1 and the total duration T are uncorrelated. More details can be found in Thejappa and Sastry (1981).

Interpretation

During periods of enhanced emission at decameter wavelengths, we observed that there can be single bursts or groups of bursts that occur at random intervals. Therefore, the simplest possible explanation for the three types of profiles presented here could be that they are due to the superposition of bursts occurring randomly in time. But it is found that the occurrence of the three types of profiles presented here is maximum only on particular days, although the period of enhanced emission may last for a much longer time. The face that the time interval ΔT defined above tends to lie in a rather narrow range, irrespective of the total duration of the burst, indicates that the profiles are not produced by entirely random superpositions of independent events. Also, the measured ratio of the amplitudes shows that the amplitudes of the initial and final phases are always a fraction of the main peak; this ratio lies between 0.1 and 0.3. This need not be the case in the case of bursts of various amplitudes occurring randomly in time.

The second possibility it that these profiles are the manifestations of fundamental-harmonic (f-h) pairs. From the work of Daigne and Moller-Pedersen (1974) and Rosenberg (1975), it is clear that the time separation between the peaks of the fundamental and harmonic emissions is, in general, constant and equal to about 4 s. It was also found that the amplitudes in f-h pairs are comparable (Rosenberg, 1975). In the present case, it is difficult to rule out the f-h pair hypothesis on the basis of the time intervals ΔT, the values of which are about the same as those found by the above authors. But the fact that the intensity ratios P_1/P and P_2/P observed by us are much less than unity does not lend support to this hypothesis. Also, according to Caroubalos et al. (1974), the ratio τ_F/τ_H of the decay constants of the fundamental and harmonic should be of the order of two if one assumes that the intensity of the fundamental $I_F \propto W$ (the energy density of plasma waves), the intensity of the harmonic $I_H \propto W^2$, and the temperatures in the regions of both fundamental and harmonic emissions are the same. Our observations show that τ_1 and τ_2 are, in general, the same and, in some cases, τ_2 can be greather than τ_1. Even if our type A and type B profiles are manifestations of f-h pairs, it is difficult to interpret type C profile on this basis. Caroubalos et al. found two clear-cut peaks in emission in the f-h pairs they studied, whereas no prominent subsidiary peak exists in the profiles presented here. Therefore, we believe that the profiles are probably not due to fundamental and harmonic emission. Zaitsev et al. (1972) have calculated the type III burst profiles by solving the one-dimensional relativistic quasi-linear equations both on a timescale $t >> \tau$, where τ is the characteristic time for the development of the two-stream instability (the time taken for plateau formation $\tau = \omega_{pe}^{-1} \frac{n}{n_s}$, where ω_{pe} is the plasma frequency, n is the density of the background plasma, and n_s is the density of electrons in the stream) and for the spatial scales $x >> L$, where L is the initial thickness of the cloud under local explosion-type initial conditions. They have shown that collisions can be neglected and only the Landau damping in the tail of the stream determines the dissipation of plasma wave energy at decameter and longer wavelengths, where the characteristic time of the absorption associated with collisions of electrons with ions in a "cold" plasma, ν_{eff}^{-1}, is much greater than the characteristic time of absorption due to Landau damping in the back of the stream, $\Delta x/V_s$ (where Δx and V_s are the extent of the stream in the corona and its mean speed, respectively) is satisfied. Their theoretical profiles agree well with experimental data in the hectometer range under the assumption that electromagnetic wave generation takes place at the second harmonic of the plasma frequency. Zaitsev et al. (1974) extended these profiles to the case where the injection time of hot electrons from the region of the flare is considerably greater than the time of existence of the burst at a given fixed frequency. The dissipation mechanism is the same Landau damping on the tail of the beam even at the decameter and meter wavelengths. The results of Zaitsev et al. (1974) have been confirmed by the extensive numerical work done by many authors (Takakura and Shibahashi, 1976; Magelsson and Smith, 1977; Grognard, 1980). The energy density of plasma waves is given by

$$W_L(\xi) = \frac{n_s \varepsilon_0}{3\sqrt{2\pi}} \frac{(\varepsilon_0/m)^{1/2}}{\nu_{eff}\ x} \left(\frac{2m\xi^2}{\varepsilon_0}\right)^3 \exp\left(-\frac{2m\xi^2}{\varepsilon_0}\right);$$

for the initial momentum distribution of the stream,

$$f_0(p) = p \frac{n_s}{\sqrt{2\pi m \varepsilon_0}} \exp(-p^2/2m\varepsilon_0).$$

The mean velocity of the beam,

$$V_s = \sqrt{\varepsilon_0/m} \quad ,$$

where n_s is the electron density in the beam, ε_0 is the initial energy of the beam, $\xi = x/t$, x is the distance between the photosphere and the respective plasma layer, m is the mass of an electron, and ν_{eff} is the effective number of collisions. The energy density reaches its maximum when

$$t = t_{max} = x\left(\frac{3}{2}\frac{\varepsilon_0}{m}\right)^{-1/2} .$$

It is possible that the profiles presented here are due to the superposition of two or three bursts caused by ordered electron beams ejected with a constant time difference. In the case of type A profiles, the electron beam responsible for the main burst should reach the appropriate plasma level soon after the electron beam causing the pre-rise leaves that level. Then the time interval ΔT is equal to the time when W_L (the plasma wave energy density), which causes the main burst, reaches its maximum. Since we know ΔT from observations, we can find the initial energy of the beam causing the main burst. From the observed ratio P_1/P, we can find the initial energy of the first beam.

If we take $x = 1.1\times10^{11}$ cm and $\Delta T = 4$ s, then $V_2 = 1.856\times10^{10}$ cm s^{-1} and $V_1 = 0.37\times10^{10}$ cm s^{-1}, where V_1 and V_2 are the mean velocities of the first and second beams. By computing the resultant time profile with the above initial energies of the beams, we are able to reproduce approximate profiles of type A and of the rise part of type C. It is not possible to reproduce the steady decay of type B and type C profiles in this manner. Note that it is possible to superpose W_L because we have used a combination of two beams that follow independent paths. It may be possible to construct all the time profiles by a combination of more than two beams. But it is not clear how the electron beams are accelerated to the above energies and ejected with constant time different.

The other possible explanation for the observed profiles is the peculiar character of the conversion mechanism of plasma waves into electromagnetic waves and their decay.

Solar Decametric Absorption Bursts

Observations. Typical examples of absorption bursts are shown in figures 2-5. A statistical analysis of several hundred absorption bursts revealed the following characteristics. (1) The absorption bursts can occur in isolation

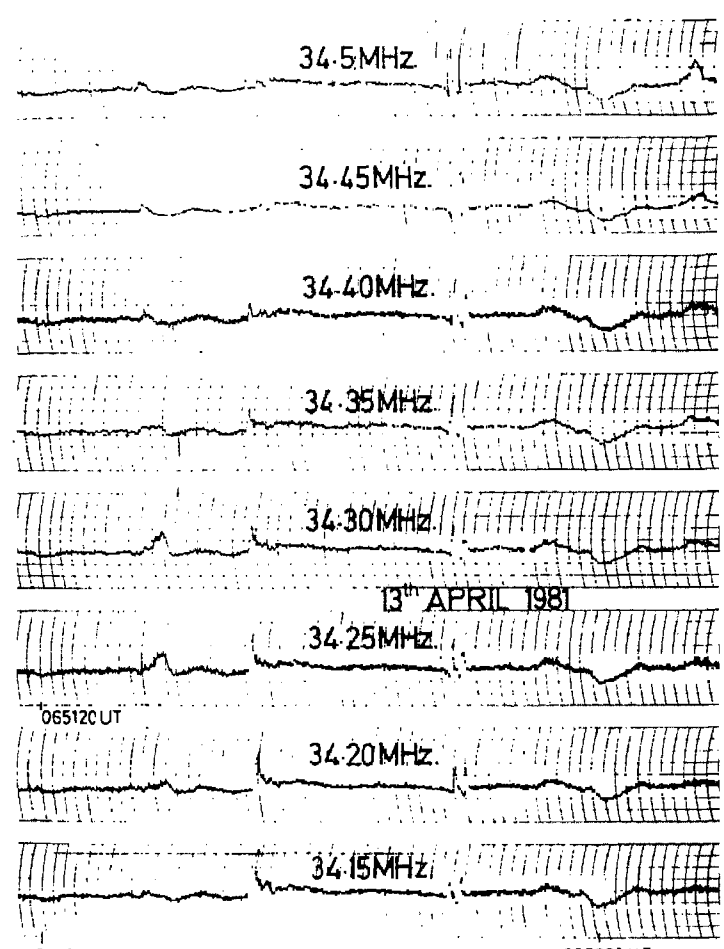

Figure 2

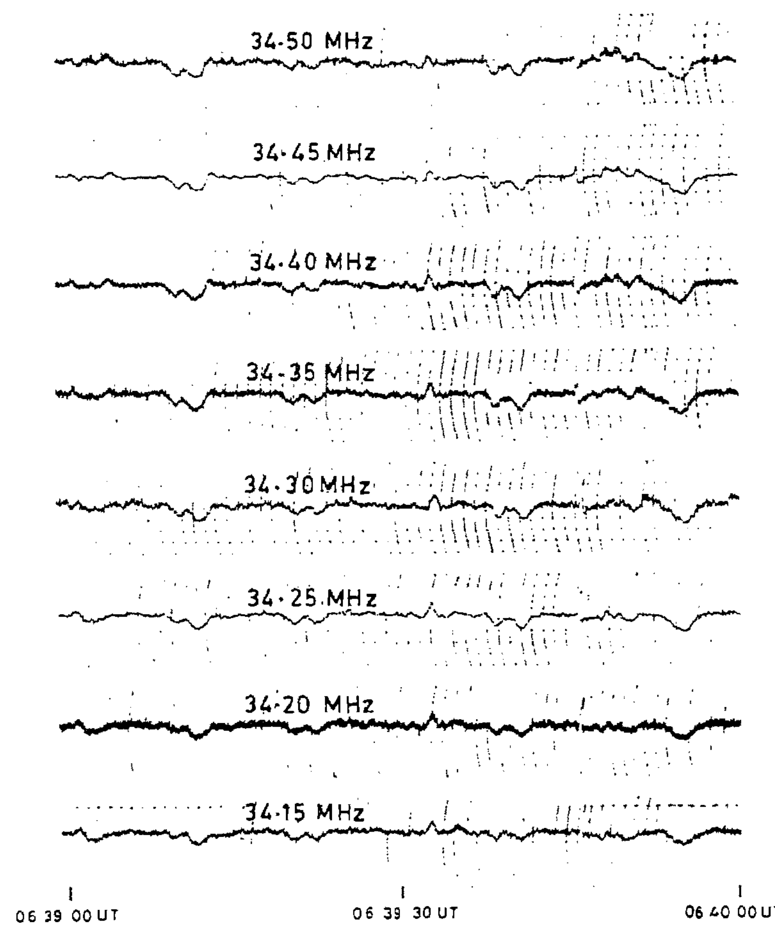

Figure 3

or can be followed or preceded by emission bursts. In some cases, absorption and emission can occur simultaneously in different frequency channels. (2) The bandwidth of absorption bursts is always greater than about 50 KHz, whereas those of emission bursts could be as narrow as 50 KHz. (3) The minimum duration of the absorption bursts is of the order of 1 s, whereas that of the emission bursts can be much smaller (100 ms). (4) The depth of the absorption is about 30-40% of the continuum level. We also noticed that, in some cases where the duration of the absorption bursts is short, the depth of absorption can be as high as 70-80% of the continuum level. These absorption bursts are discussed in detail by Sastry et al. (1983) and by Gopalswamy (1983).

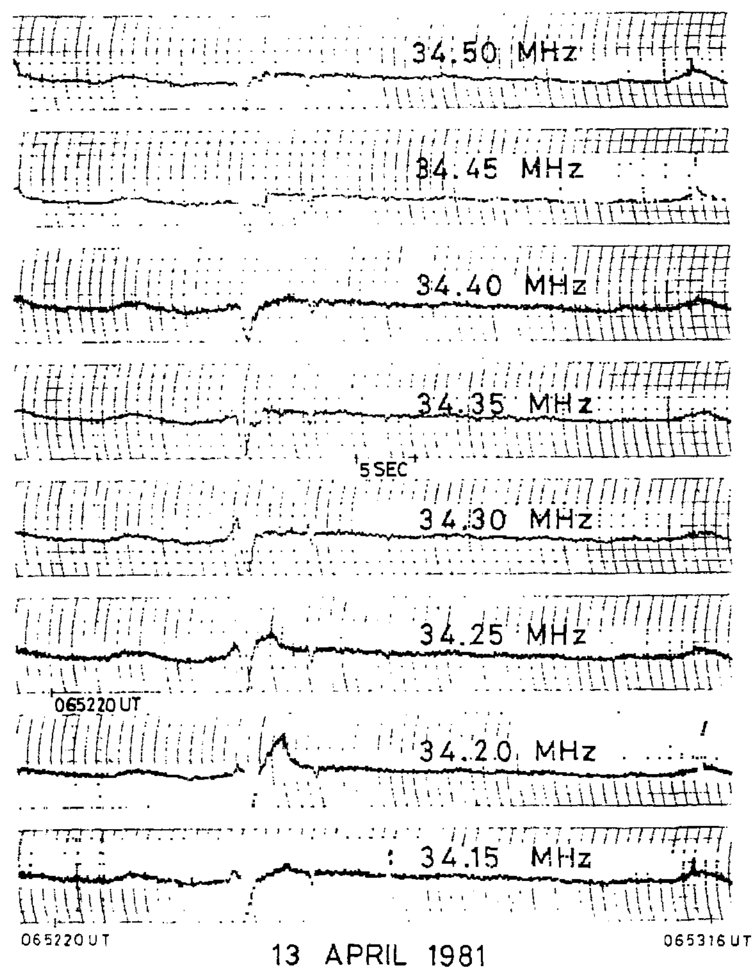

Figure 4

A Suggested Explanation. Benz and Kuijpers (1976) believe that the sudden reductions in the type IV decimetric continuum are due to the quenching of the loss-cone instability by electron streams. Fokker (1982) proposed that the continuum radiation is ducted through open magnetic flux tubes and that the radiation is screened by inhomogeneities created on the path of the radiation by lateral shock waves or solitons impinging on the flux tubes. So, following Fokker (1982), we assume that even the decametric continuum radiation is absorbed on its path rather than at the generation stage.

We propose the following scenario for the observed absorption bursts. A shock propagates perpendicularly to the magnetic field just above the continuum source. The perpendicular currents due to the shock gradients generate ion-acoustic turbulence in the shock front and in its wake. When the continuum radiation passes through the region of

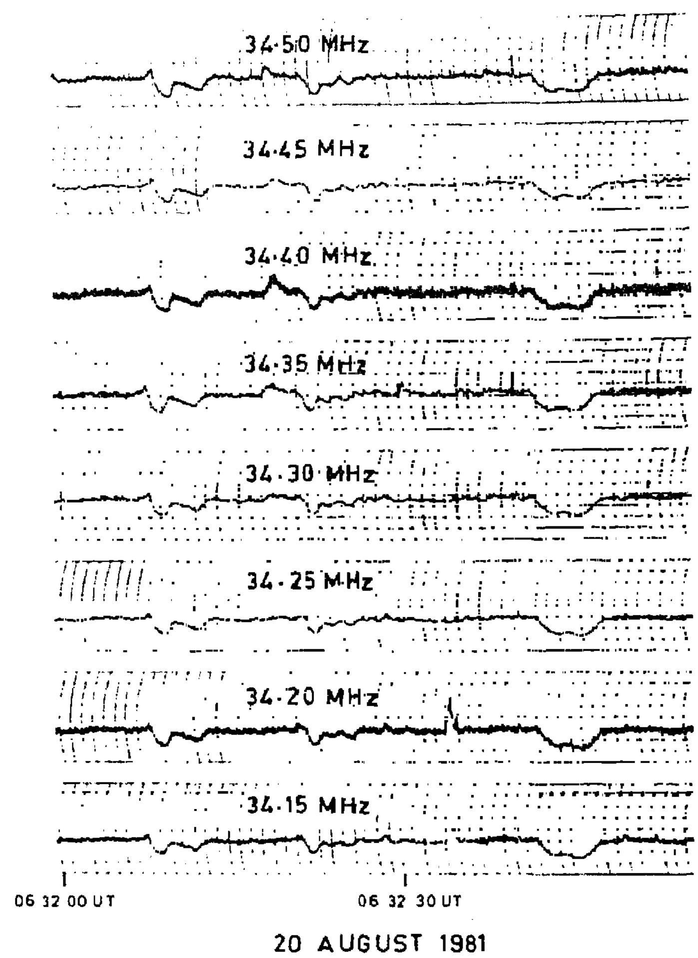

Figure 5

ion-acoustic turbulence, a three-wave interaction occurs: $t \rightarrow \ell \pm s$, where t indicates transverse waves, s ion-acoustic waves, and ℓ Langmuir waves. A theoretical analysis of the above process for the decametric levels shows that the required effective temperature of the ion-acoustic turbulence $\langle T_s \rangle > 2.5\times10^9$ K. The calculated fractional bandwidth, $B = (\Delta\omega/\omega) = (3/2)(\langle\omega_s\rangle/\omega_{pi})$, is the in the same range as the observed fractional bandwidth, 5×10^{-2}, and the thickness of the absorbing layer, $L \simeq 10^9$ cm. (ω_{pi} is the ion plasma frequency and ω_s is the ion-acoustic frequency). The duration of the absorption could be attributed to the period during which the ion-acoustic turbulence exists above the critical level given above. Gopalswamy et al. (1983) have discussed the above model in detail.

Slowly Drifting Spike Bursts

Observations. Typical examples of decametric slow drifting spike bursts are presented in figures 6 and 7: (1) the

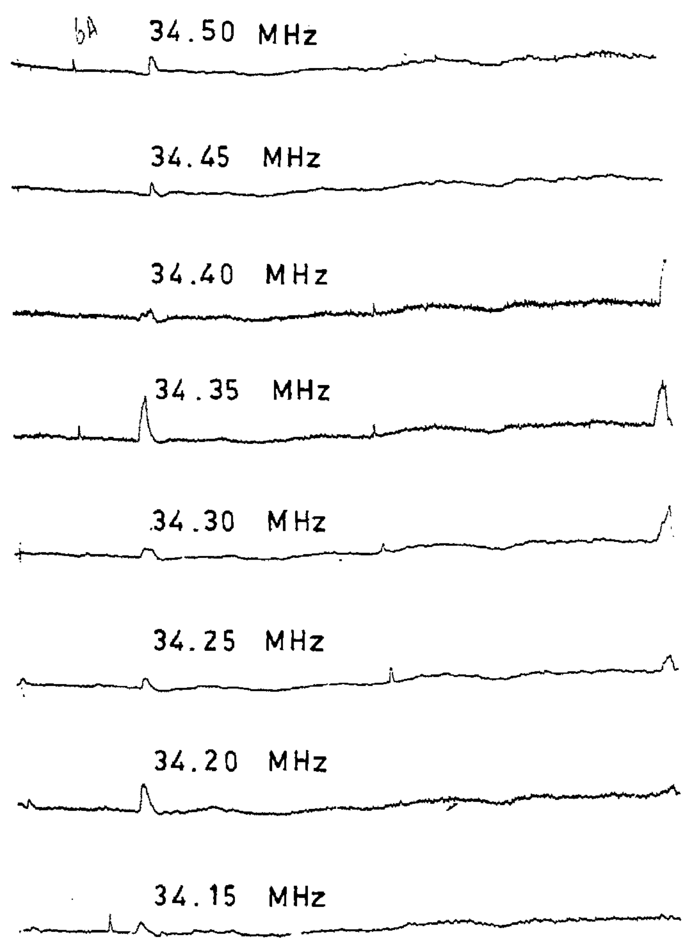

Figure 6

single frequency duration is about 300 ms, (2) the relative bandwidth is about 3%, (3) the drift rate is about 250 KHz/s, which corresponds to a velocity for the exciting agency of 2.6×10^7 cm s^{-1}, (4) the single frequency duration increases systematically towards lower frequencies, and (5) bursts are superposed over a weak continuum.

Interpretation. The short-duration narrow-band character is similar to S-bursts (McConnel, 1980). However, the drift rate is similar to that of type II. But frequency and bandwidth characteristics rule out type II. Moreover, no flare association is seen. Therefore, one can definitely

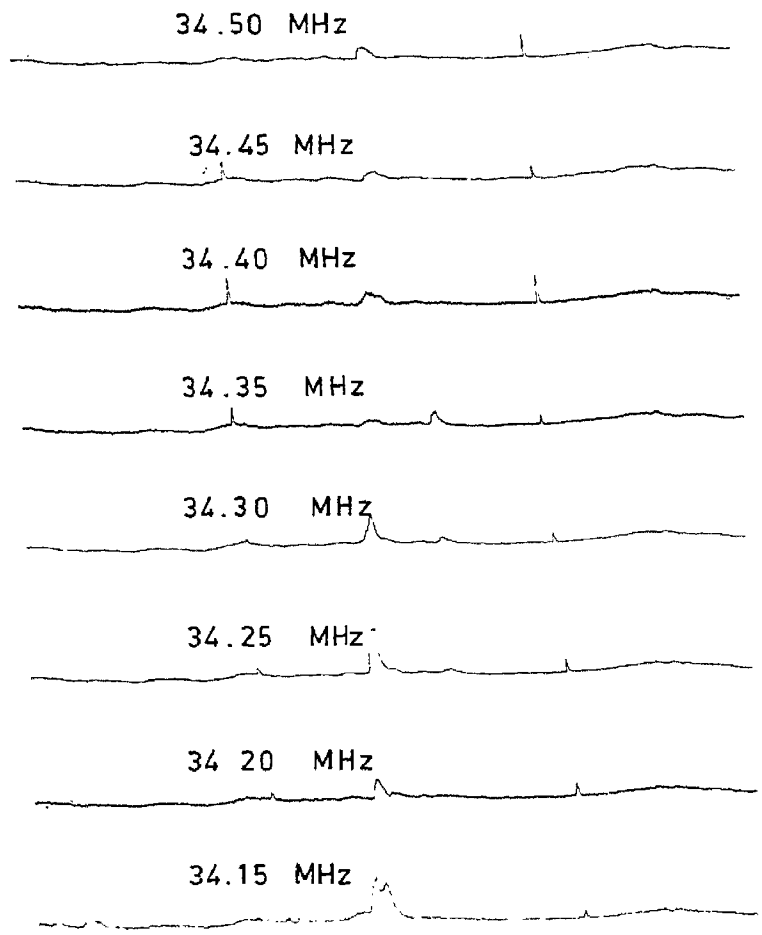

Figure 7

say that these are slowly drifting type I bursts at the decametric level. The drift velocity, 2.6×10^{7} cm s^{-1}, rules out the possibility of an electron stream as a source because $V_{sound} < V_{thermal}$. Calculations show that the observed features are not due to the dispersion of the medium either. So the only agency that can generate the observed spikes is a weak shock. The shocks generate low-frequency turbulence, which, in turn, produces the loss-cone distribution of hot particles. Upper hybrid (UH) turbulence is generated by loss-cone anisotropy. There is a good overlap in k-space for upper-hybrid and low-frequency waves. Therefore, the interaction between UH and low-frequency waves produces the observed spikes. Lower-hybrid (LH) waves and ion-acoustic waves are the two possible candidates for low-frequency waves. Gopalswamy et al. (1983) have shown that ion-acoustic waves have a better overlap in k-space with UH waves and that they have a higher saturation energy density than LH waves (more than two orders of magnitude).

The observed bandwidth and drift velocity of the bursts can be used to estimate the coronal magnetic field with the aid of Rankine-Hugoniot (RH) relations for perpendicular shocks. The bandwidth of the observed bursts is very small; this is the case for most of the type I bursts (Elgaroy, 1977). Therefore, one can relate the relative bandwidth to the relative density jump ($\Delta n/n$) across the shock as follows. Since

$$\omega_{pe} = \left(\frac{4\pi e^2}{m}\right)^{1/2} \sqrt{n} ,$$

one can write

$$\frac{\Delta\omega_{pe}}{\omega_{pe}} = -\frac{1}{2}\frac{\Delta n}{n} .$$

Since the observed bandwidth is 3%, $\Delta n/n$ must be 6%. From the RH relation (Tidman and Krall, 1971),

$$\frac{\Delta n}{n} = \frac{\Delta B}{B} = 1 - \frac{1}{8}\left\{\left(\frac{5C_s^2}{V_1^2} + 1 + \frac{5V_A^2}{2V_1^2}\right) + \left[\left(\frac{5C_s^2}{V_1^2} + 1 + \frac{5V_A^2}{2V_1^2}\right)^2 + \frac{8V_A^2}{V_1^2}\right]^{1/2}\right\} ,$$

we obtain

$$\frac{V_A^2}{V_1^2} = \frac{8\left(1 - \frac{\Delta n}{n}\right)^2 - 2\left(1 - \frac{\Delta n}{n}\right)\left(1 + \frac{5C_s^2}{V_1^2}\right)}{1 + 5\left(1 - \frac{\Delta n}{n}\right)} ,$$

where V_A is the Alfvén velocity, C_s is the ion sound velocity, V_1 is the shock velocity, and $\Delta B/B$ is the magnetic field jump. Since $C_s = 9\times10^6$ cm s^{-1} and $V_1 \doteq 2.6\times10^7$ cm s^{-1}, we get $V_A = 2.19\times10^7$ cm s^{-1}. Using the relation

$$V_A = \frac{B}{\sqrt{4\pi n m_i}} ,$$

we get $B \simeq 1G$. This value is in very good agreement with other estimates ($\sim 1G$) such as frequency splitting and polarization measurements of type I bursts (ter Haar and Tsytovich, 1981).

CONCLUSIONS

The decametric region of the solar corona is very interesting from the viewpoint of a plasma physicist. The smooth transition from a type I noise storm to a type III noise storm occurs. This is the most probable region in which closed magnetic loops could give way to open field configurations. Moreover, the corotation of the corona ceases and the solar wind originates in this region. There is not much theoretical work regarding the variety of processes taking place in this region. We hope that the present paper has brought to light the importance of the study of plasma processes in the decametric corona. Theories regarding the time evolution of various nonlinear processes could be tested using our observations.

ACKNOWLEDGMENT

One of the authors (G.T.) is grateful to J. C. Bhattacharyya for encouragement and thanks the organizers of the Kiev Workshop for their hospitality.

REFERENCES

Aubier, M. and Boischot, A. (1972), *Astr. Astrophys.*, 19, 343.
Benz, A. O. and Kuijpers, J. (1976), *Solar Phys.*, 46, 275.
Caroubalos, C., Poquerusse, M. and Steinberg, J. L. (1974), *Astr. Astrophys.*, 32, 255.
Daigne, G. and Moller-Pedersen, B. (1974), *Astr. Astrophys.*, 37, 355.
Elgaroy, O. (1977), *Solar Noise Storms*, Pergamon, Oxford.
Fokker, A. D. (1982), *Solar Phys.*, 77, 255.
Gopalswamy, N., Thejappa, G. and Sastry, Ch. V. (1983a), *J. Astrophys. Astr.*, 4, 215.
Gopalswamy, N., Thejappa, G., Subramaniam, K. R. and Sastry, Ch.V. (1983b), Communicated to *Solar Phys.*
Grognard, R. J. M. (1980), in *IAU Symp. 86: Radio Physics of the Sun*, Eds. M. R. Kundu and T. E. Gergely, D. Reidel, Dordrecht, p. 303.
Magelsson, G. R. and Smith, D. F. (1977), *Solar Phys.*, 55, 211.
McConnel, D. (1982), *Solar Phys.*, 78, 253.
Rosenberg, H. (1975), *Solar Phys.*, 42, 247.
Sastry, Ch. V. (1969), *Solar Phys.*, 10, 429.
Sastry, Ch. V. (1971), *Astrophys., Lett.*, 8, 115.

Sastry, Ch. V. (1972), *Astrophys., Lett.*, 11, 47.
Sastry, Ch. V. (1973), *Solar Phys.*, 28, 187.
Sastry, Ch. V., Subramanian, K. R. and Krishan, V. (1983), *Astrophys., Lett.*, 23, 95.
Slottje, C. (1972), *Solar Phys.*, 25, 210.
Slottje, C. (1978), *Nature*, 256, 520.
Takakura, T. and Shibahashi, H. (1976), *Solar Phys.*, 46, 323.
ter Haar, D. and Tsytovich, V. N. (1981), *Phys. Rep.*, 73, 175.
Thejappa, G. and Sastry, Ch. V. (1982), *J. Astrophys. Astr.*, 3, 151.
Tidman, D. A. and Krall, N. A. (1971), *Shock Waves in Collisionless Plasmas*, Interscience, New York.
Zaitsev, V. V., Kunilov, M. V., N. A. Mityakov and Rapoport, V. O. (1974), *Sov. Astr.*, 18, 147.
Zaitsev, V. V., Mityakov, N. A. and Rapoport, V. O. (1972), *Solar Phys.*, 24, 444.